

Original Article

microRNA-203 functions as a natural Ras inhibitor in hepatocellular carcinoma

Jun Guo^{1*}, Lei Li^{2*}, Nan Deng², Yong Xu², Guohua Wang³, Hongbo Luo⁴, Chuanrui Xu², Xiaolei Li⁵

¹Department of Pharmacy, Tongji Hospital, Tongji Medical College, Huazhong University of Science and Technology, Wuhan 430030, Hubei, China; ²School of Pharmacy, Tongji Medical College, Huazhong University of Science and Technology, Wuhan 430030, Hubei, China; ³Department of Hepatobiliary Surgery, The Second Hospital of Wuhan Iron and Steel Corp, Wuhan 430030, Hubei, China; ⁴Department of Urology, Renmin Hospital of Wuhan University, Wuhan 430030, Hubei, China; ⁵Department of Thyroid and Breast Surgery, The 960th Hospital of The PLA, Jinan 250031, Shandong, China. *Co-first authors.

Received September 28, 2022; Accepted February 19, 2023; Epub April 15, 2023; Published April 30, 2023

Abstract: microRNA-203 (miR203) plays an important role in the formation and development of multiple types of cancers. However, its role in hepatic carcinogenesis has not been well studied. Mitogen-activated protein kinase signaling is known to be activated in hepatocellular carcinoma (HCC), but there is a lack of effective drugs targeting this pathway for HCC treatment. In this study, we investigated the role of miR203 in HCC and the underlying mechanism. We found that miR203 was significantly downregulated in HCC cell lines and patient tissues compared with a hepatocyte cell line (L02) or normal liver tissues. Restoration of miR203 inhibited HCC cell growth and induced cell cycle arrest and apoptosis. In primary and xenograft HCC mouse models, miR203 also significantly blocked HCC growth. Bioinformatic analysis indicated that miR203 directly binds to the 3'UTR of NRas mRNA, resulting in decreased expression of NRas and inactivation of mitogen-activated protein kinase (MAPK) signaling. Activation of MAPK signaling by ectopic NRas expression rescued the cell proliferation blocked by miR203. Together, our findings illustrate the fundamental role of miR203 as a natural inhibitor of RAS/MAPK signaling in hepatic carcinogenesis *in vitro* and *in vivo*. In light of the critical and universal activation of the MAPK pathway in HCC, miR203 has the potential to serve as a nucleotide drug for the treatment of HCC with activated MAPK signaling.

Keywords: microRNA-203, hepatocellular carcinoma, Ras, mitogen activated protein kinase

Introduction

HCC is the most common form of liver cancer and the third leading cause of cancer-related death, with more than 700,000 new patients diagnosed per year worldwide [1]. Risk factors for HCC include chronic hepatitis B and C viral infection, chronic alcohol consumption, aflatoxin-B1-contaminated food, and various cirrhosis-inducing conditions [2, 3]. Although hepatitis B (HBV) and C (HCV) infection are the major risk factors for HCC, nonalcoholic fatty liver disease (NAFLD) and NASH contribute to HCC development and are becoming an increasingly common cause of HCC worldwide [4]. A projection study indicates that in the 30 selected countries, by 2030, there will be a 35% increase in the future number of new cases of primary liver cancer annually, from 339,000 in 2005

to over 459,000 in 2030 [5]. Despite the increasing incidence of HCC worldwide, treatment options for unresectable HCC are limited. To date, only sorafenib and lenvatinib have been approved as first-line drugs for patients with unresectable HCC, and regorafenib, cabozantinib and ramucirumab have been approved for second-line treatment [6]. However, these agents showed limited benefits and are associated with considerable toxicities and poor quality-of-life outcomes. Recently, the phase III IMbrave150 trial results showed that combining an anti-PDL1 antibody with an anti-VEGFA antibody leads to promising efficacy for advanced HCC patients [7]. Currently, this combination of immunotherapy has become the first-line treatment strategy against HCC [8]. Nevertheless, most patients eventually progress with combination immunotherapy. There-

fore, studies to elucidate the molecular mechanisms underlying HCC pathogenesis and to seek more effective drugs for precision medicine are still needed.

The Ras/MAPK pathway plays a fundamental role in the malignant transformation and progression of HCC [9]. MEK and ERK proteins are increased and phosphorylated in HCC [10]. One histological study indicated that overexpression and phosphorylation of MAPK were detected in 91% (42 of 46) and 69% (32 of 46) of HCCs examined, respectively [11]. Accumulating data further demonstrate that most human HCCs harbor overexpression and/or activation of MEK 1/2 and ERK 1/2 compared to surrounding nonneoplastic liver tissue [12, 13]. Treatment of HCC cells with a specific MEK inhibitor leads to growth inhibition and apoptosis, pointing to a key role of the MAPK pathway in HCC cell survival and tumor growth. In addition to MEK and ERK inhibitors, Ras inhibitors have been pursued for several decades and were not obtained until recent years due to the “undruggable” structure of Ras [14, 15]. Approval of the first Ras (G12C) inhibitor sotorasib (AMG510) for non-small cell lung cancer (NSCLC) treatment proved that targeting mutated Ras is possible and paved a new way for targeting MAPK signaling [16, 17]. In HCC, however, Ras is seldom mutated, but the MAPK pathway remains activated. Therefore, blockade of unmutated Ras or activation of MAPK signaling should be aims of HCC treatment.

MicroRNAs (miRNAs) are small noncoding RNAs that function as master regulators of gene expression, and dysregulated miRNAs play critical roles in tumor initiation and progression in many types of cancers. Of them, downregulation of miR203 has been reported in various tumors, including cervical cancer, prostate cancer, gastric cancer and bladder cancer [18-22]. Other studies have also indicated that miR203 is upregulated in metastatic breast cancers and chemotherapy-resistant colon cancers [23, 24]. Previously, we screened miRNA expression in HCC mouse models and found that miR203 was downregulated in addition to miR101 and miR375 [25]. Since roles of miR101 and miR375 have been reported, we then focused on miR203 and found that miR203 is significantly downregulated in HCC cell lines as well. However, its role in hepatic

carcinogenesis remains unclear. Therefore, we explored the role of miR203 in HCC formation and development and uncovered its working mechanism in this study.

Materials and methods

Establishment of AKT/Ras, AKT/h-Met and c-Myc HCC mouse models

Five-week-old female C57BL/6 mice were purchased from Charles River Technology Corporation (Beijing, China), and all mice were fed standard rodent chow in the experimental animal center of Tongji Medical College, Huazhong University of Science and Technology. Plasmids used for hydrodynamic injections to establish HCC mouse models were provided by Dr. Xin Chen (University of California, San Francisco), including pT3-EF1 α -AKT, pCaggs-NasV12, pT3-EF1 α -h-Met, pT3-EF1 α -c-Myc, and pCMV-SB. Hydrodynamic transfection was performed as described [26]. For AKT/Ras-induced HCC, mice (n = 5) were hydrodynamically injected with 5 μ g of pT3-EF1 α -AKT and 5 μ g of pCaggs-NasV12 together with 1 μ g of pCMV-SB. For AKT/h-Met-induced HCC, mice (n = 5) were hydrodynamically injected with 5 μ g of pT3-EF1 α -AKT and 5 μ g of pT3-EF1 α -h-Met together with 1 μ g of pCMV-SB. For c-Myc-induced HCC, mice (n = 5) were hydrodynamically injected with 5 μ g of pT3-EF1 α -c-Myc together with 1 μ g of pCMV-SB. Saline-injected mice (n = 5) were used as controls. Different groups of plasmids were mixed and diluted in 2 mL of saline and filtered through a sterile 0.22- μ m filter. Then, the solution was injected into the lateral tail vein of mice in 5-7 seconds. All mice were weighed, and their vitality was monitored every 4 days. Tumor development was observed by abdominal palpation and indicated indirectly by mouse weight. Mice were sacrificed by cervical dislocation after CO₂ euthanasia at the terminal time point of tumor burden. All mice were monitored in accordance with protocols approved by the committee for animal research at Tongji Medical College, Huazhong University of Science and Technology.

Cell culture and lentiviral infection

Human HCC cell lines, including HepG2, Huh7, and Hep3B, were purchased from the China Center for Type Culture Collection at Wuhan University (Wuhan, China) and stored in our

miR-203 inhibits hepatocellular carcinoma by targeting NRas

ethanol overnight and stained using a Cell cycle staining Kit (MultiSciences, 70-CCS012), including propidium iodide (staining solution: 0.04 mg/mL propidium iodide (Sigma-Aldrich) and 0.1 mg/mL ribonuclease A from bovine pancreas (RnaseA, Sigma-Aldrich)). The cell cycle was analyzed using flow cytometry (Cytomics™ FC 500; Beckman Coulter, Brea, CA, USA), and the results were analyzed using FlowJo7.6 (FlowJo, Ashland, OR, USA).

Protein extraction and Western blotting

Proteins were extracted from cells or mouse liver tissues by M-PER Mammalian Protein Extraction Buffer (Thermo Fisher Scientific) containing Proteinase Inhibitor Cocktail (Roche, Indianapolis, IN, USA) and Halt Phosphatase Inhibitor Cocktail (Thermo Fisher Scientific). Then, the supernatants were harvested after centrifugation at 4°C and 12000 × g for 10 min. Protein concentration was quantified using the Pierce BCA Protein Assay Kit (Thermo Fisher Scientific) and denatured by boiling with 5 × SDS loading buffer (125 mmol/l Tris-HCl, 4% SDS, 20% glycerol, 100 mmol/l DTT, and 0.2% bromophenol blue) at a ratio of 1:4. Proteins were then loaded on 10-15% SDS-polyacrylamide gels. The separated proteins were then transferred onto polyvinylidene difluoride membranes. The membranes were blocked in 5% defatted milk at room temperature for 1 h and incubated with primary antibodies at 4°C overnight. Membranes were then washed and incubated with horseradish peroxidase-conjugated secondary antibody at room temperature for 1 h. Protein antigens were stained with Pierce™ ECL Western blotting Substrate (Thermo, USA) and visualized by enhanced electrochemiluminescence Western blot substrate detection (Pierce). All experiments were repeated at least three times. All antibodies used are listed in [Table S2](#).

Xenograft HCC mouse model

For the xenograft HCC tumor model, Hep3B cells were first stably transfected with LV3-Plenti-CMV-puromycin-miR203 (LV3-miR203) or scramble vector (LV3-SC). Twenty-four hours after transfection, cells were harvested and counted for density. Six-week-old BALB/c athymic nude female mice (Charles River, Beijing, China) were subcutaneously injected in the right flank with 8×10^6 Hep3B-LV3-miR203

cells or Hep3B-LV3-SC cells resuspended in 0.1 mL of phosphate-buffered saline (n = 7 in each group). All mice were fed under specific pathogen-free conditions. Body weight and tumor volume were measured every 4 days. Tumor volume was measured with Vernier calipers and calculated as $V = \text{length} \times \text{width}^2 \times 0.52$. Mice were sacrificed by cervical dislocation after CO₂ euthanasia when the maximal tumor volume reached 2000 mm³, and tumors were isolated and weighed. All mice were monitored in accordance with protocols approved by the committee for animal research at Tongji Medical College, Huazhong University of Science and Technology.

Construction of the miR203 expression vector

We generated a versatile expression vector of miR203 according to Golden Gate cloning instructions [25]. A 400-base-pair fragment containing the human miR203 precursor was amplified from human genomic DNA and then inserted into a pT3-EF1α (elongation factor 1 alpha) vector, referred to as pT3-EF1α-miR203. To determine the inhibitory effect of miR203 on AKT/Ras-induced HCC, mice (n = 15) were hydrodynamically injected with 5 μg of pT3-EF1α-AKT, 5 μg of pCaggs-NasV12 and 20 μg of pT3-EF1α-miR203 together with 1.2 μg of pCMV/SB. Control mice (n = 15) were injected with 5 μg of pT3-EF1α-AKT, 5 μg of pCaggs-NasV12 and 1 μg of pCMV/SB. To evaluate the effect of miR203 on AKT/h-Met-induced HCC, mice (n = 15) were hydrodynamically injected with 5 μg of pT3-EF1α-AKT, 5 μg of pT3-EF1α-h-Met and 20 μg of pT3-EF1α-miR203 together with 1.2 μg of pCMV/SB. Control mice (n = 15) received 5 μg of pT3-EF1α-AKT, 5 μg of pT3-EF1α-h-Met and 0.4 μg of pCMV/SB. Mice were monitored every 4 days and sacrificed at 6 or 7 weeks post injection for histological examination and further evaluation.

Histology and immunohistochemistry

Mice were euthanized, and liver tissues were dissected out and rinsed with saline. Aliquots of samples were fixed with 4% paraformaldehyde at 4°C overnight. The samples were paraffin-embedded and cut into 5-μm sections for hematoxylin and eosin (H&E) or immunohistochemical (IHC) staining. Paraffin sections were reacted with antibodies (appropriate dilution)

and then stained with rabbit serum instead of the target antibody as a negative control. Cells exhibiting positive staining on cell membranes and in the cytoplasm and nucleus were counted in at least 10 representative fields ($\times 200$ magnification). All antibodies used for IHC are listed in [Table S2](#).

Prediction of miR203 targets

Prediction of miR203 target genes was conducted as reported previously [27]. The target gene databases of miR203 were downloaded from the TargetScan database. The hits from TargetScan were confirmed by high-throughput sequencing of RNAs isolated by cross-linking immunoprecipitation (HITS-CLIP) from the Argonaute protein complex (Ago HITS-CLIP). We then carried out Gene Ontology analysis using PathwayStudio software (Elsevier, Amsterdam, Netherlands).

Luciferase reporter assay

The NRas 3'-UTR containing the wild-type or mutated miR203-3p binding sequences was synthesized by GeneCreate (Wuhan, China) and cloned into the pmirGLO luciferase reporter vector (Promega, Madison, WI, USA). Briefly, Hep3B cells were cultured at a density of 2×10^4 cells/well in 96-well plates and transfected with 0.2 μg of dual luciferase reporter construct p1 or cotransfected with 0.2 μg of the luciferase reporter construct p2 and the internal control vector pRL TK, pRL SV40, or pRL-CMV (Promega, Madison, WI, USA) at a ratio of 20:1 (reporter construct: control vector) using LipofectamineTM 2000 (Invitrogen) according to the manufacturer's instructions. Six hours post transfection, the transfection medium was removed and replenished with medium containing 6 μM curcumin (Sigma Aldrich, St. Louis, MO, USA) solubilized in 100% dimethyl sulfoxide (DMSO, Sigma). Forty-eight hours post transfection, the luciferase activity was measured using the Dual Luciferase[®] Reporter Assay System (Promega). Renilla luciferase activity was normalized to firefly luciferase activity in cells transfected with the dual luciferase reporter construct p1, and firefly luciferase activity was normalized to Renilla luciferase activity in cells cotransfected with the reporter construct p2 and the control vector.

Statistical analysis

GraphPad Prism Software (La Jolla, CA, USA) was used for statistical analyses. All values are depicted as the mean \pm standard error of the mean (SEM) and were considered significant if $P < 0.05$. The data were analyzed by Student's t test or one-way ANOVA. All experiments were repeated at least three times.

Results

MiR203 is downregulated in HCC, and a high level of miR203 is related to longer survival of HCC patients

To identify whether miR203 plays an important role in the development of HCC, we examined miR203 levels in three HCC mouse models, AKT/Ras-, AKT/h-Met-, and c-Myc-induced HCC. The results indicated that miR203 was expressed at lower levels in mouse HCC tissues than in normal liver tissues (**Figure 1A**). miR203 levels were also examined in HepG2, Huh7, and Hep3B cells, and the results showed that miR203 levels were lower in HCC cells than in L02 cells (**Figure 1B**). GEO datasets showed that miR203 levels were reduced in human HCC specimens compared with normal liver tissues (**Figure 1C**). Survival analysis of HCC patients with high or low miR203 levels revealed that patients with high miR203 levels survived longer than those with low miR203 levels (**Figure 1D, 1E**). Together, these results indicated that miR203 is downregulated during hepatic carcinogenesis and that a lower level of miR203 is a prognostic marker for shorter survival.

MiR203 inhibits HCC cell proliferation and blocks cell cycle progression in vitro

To identify the role of miR203 in HCC, HepG2, Huh7, and Hep3B cells were transfected with miR203-expressing lentivirus for 72 h. qRT-PCR results showed that miR203 levels were significantly increased in these three HCC cell lines after transfection (**Figure 2A**). CCK-8 assays showed decreased cell viability in HepG2, Huh7 and Hep3B cells transfected with miR203 lentivirus (LV3-miR203) compared with the negative control (LV3-SC) after 4 days of culture (**Figure 2B**). Cell counting indicated that the proliferation of HCC cells was

miR-203 inhibits hepatocellular carcinoma by targeting NRas

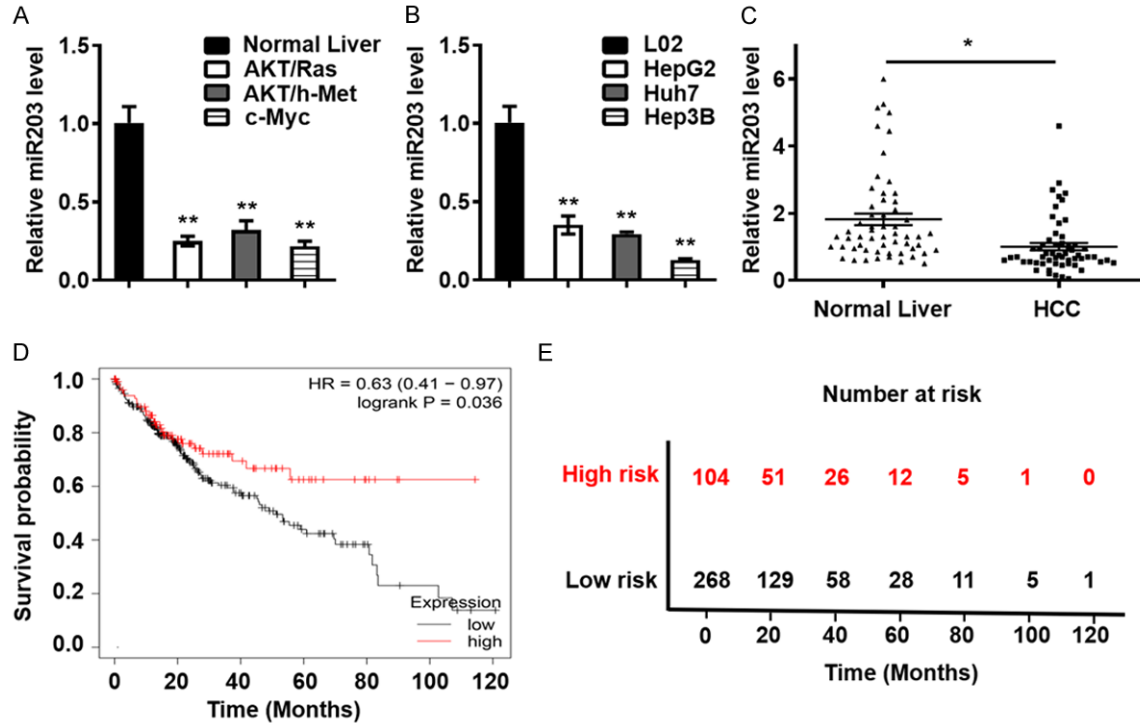


Figure 1. The expression of miR203 is downregulated in HCC. A. Reduced expression of miR203 in the livers of AKT/Ras-, AKT/h-Met-, and c-Myc-induced HCC mouse models compared with normal mice determined by using qRT-PCR. n = 5 in each group. B. Relative miR203 levels in human HCC cell lines with different genetic backgrounds compared with L02 cells detected using qRT-PCR. C. Downregulation of miR203 in human HCC tissues (n = 57) versus normal liver tissues (n = 57). Data were extracted from the GEO database (accession no: GSE67139). D, E. Survival analysis of HCC patients with high miR203 expression (n = 199) and patients with low miR203 expression (n = 500). Data were from the GEO database (GSE119221). The data were analyzed by Student's t test or one-way ANOVA to evaluate the statistical significance, and the results are presented as the mean \pm SD. *P < 0.05; **P < 0.01.

suppressed by restoration of miR203 (**Figure 2C**). Notably, sustained expression of miR203 significantly impaired colony formation of HCC cells (**Figure 2D**). In addition, cell cycle analysis suggested that miR203 intercepted cell cycle progression and significantly delayed the G2/M phase of the cell cycle (**Figure 2E**). Finally, cell cycle arrest was confirmed by Western blotting (**Figure 2F**), and the expression of all relative proteins was quantified (**Figure S1**). Collectively, these results corroborated the idea that miR203 inhibits the proliferation of human HCC cell lines.

MiR203 suppresses the growth of HCC xenograft tumors

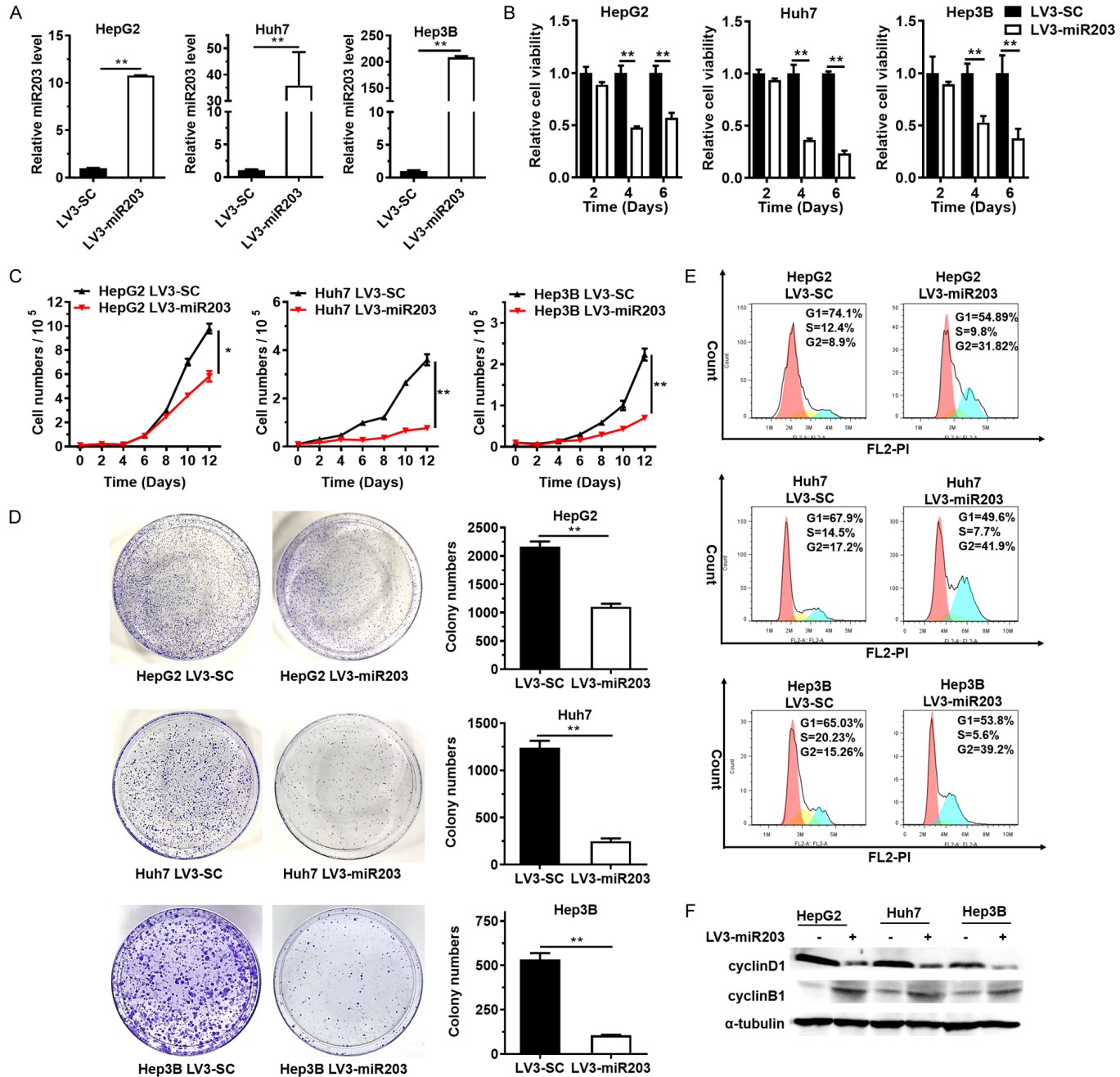
To clarify whether miR203 represses the development of HCC *in vivo*, Hep3B cells transfected with LV3-SC or LV3-miR203 lentivirus were allografted into subcutaneous tissues of

6-week-old nude mice. Consistent with the inhibitory effects *in vitro*, miR203 robustly attenuated the growth of HCC xenografts (**Figure 3A**). Consistently, mouse body weights were decreased, and tumor weights and tumor volumes were significantly decreased in the LV3-miR203 mice (**Figure 3B-D**). qRT-PCR confirmed the overexpression of miR203 in LV3-miR203 tumors (**Figure 3E**). These data collectively suggested that miR203 exerts a tumor suppressive role in HCC development.

MiR203 blocks HCC initiation and development in primary HCC mouse models

In our previous study, we reported that activation of AKT/Ras or AKT/h-Met can induce HCC in mice at 4-6 weeks [28]. Coordinated activation of AKT/mTOR and Ras/MAPK cascades occurs in over 50% of all human HCCs [29], and coactivation of AKT and c-Met is also frequently

miR-203 inhibits hepatocellular carcinoma by targeting NRas



miR-203 inhibits hepatocellular carcinoma by targeting NRas

Figure 2. miR203 inhibits HCC cell proliferation *in vitro*. A. Upregulation of miR203 by lentivirus in human HCC cell lines with divergent backgrounds. B. Viability of HCC cells treated with miR203 lentivirus (LV3-miR203) or scrambled lentivirus (LV3-SC) using a CCK-8 kit. C. Cell proliferation curves of LV3-miR203-infected HCC cell lines compared to LV3-SC-infected cells. D. Soft agar colony formation of HepG2, Huh7, and Hep3B cells transfected with LV3-miR203 or LV3-SC. E. Cell cycle distribution in HCC cells treated with LV3-miR203 lentivirus or control lentivirus by flow cytometry (FCM). F. Expression of the cell cycle-related proteins cyclin D1 and cyclin B1 using Western blotting. Data are presented as the mean \pm SD, $n = 3$ per group, $**P < 0.01$.

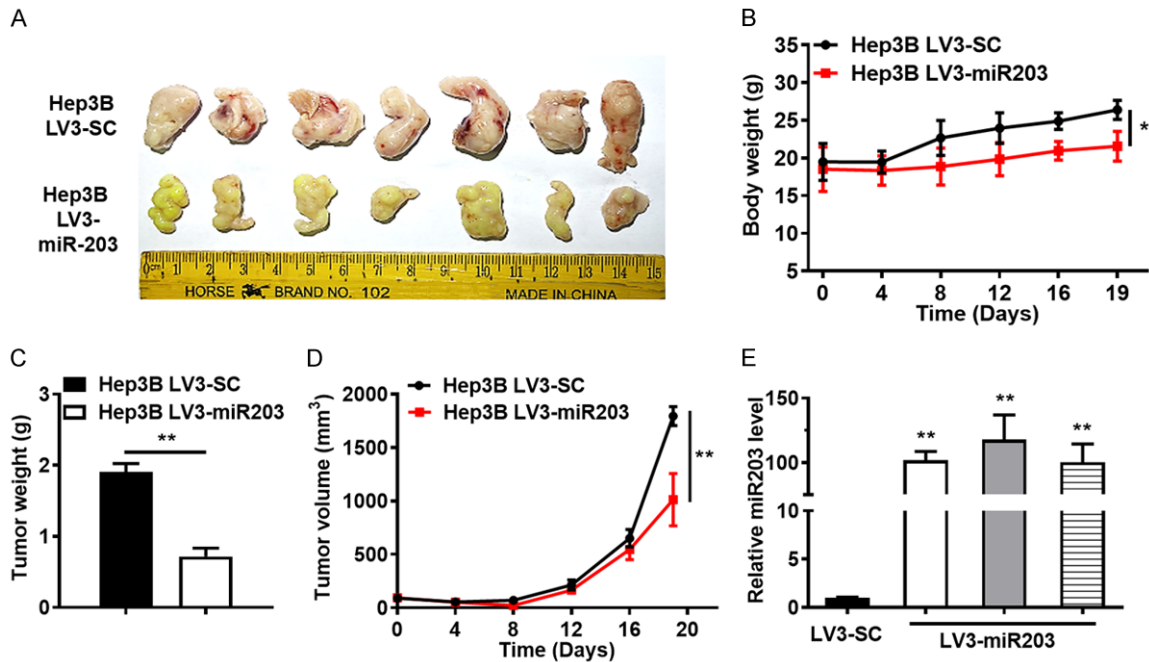


Figure 3. miR203 suppresses the growth of HCC xenograft tumors. A. Gross images of xenografts induced by Hep3B cells that were stably transfected with LV3-miR203 ($n = 7$) or LV3-SC ($n = 7$). B. Mouse body weight curve in two different groups. C, D. Weight and growth curve of HCC xenograft tumors in each group. E. miR203 level in each group by qRT-PCR. Data are presented as the mean \pm SD, $n = 7$ per group, $*P < 0.05$, $**P < 0.01$.

observed in HCC patients [28]. Thus, we investigated the effect of miR203 in AKT/Ras and AKT/h-Met HCC mice. Mice in the AKT/Ras group died from lethal tumor burdens by 4-6 weeks postinjection, with livers covered in HCC lesions (Figure 4A). In contrast, AKT/Ras/miR203 group mice harbored minor and less proliferative HCC nodules (Figure 4B). Moreover, miR203 prolonged the survival of HCC mice to nearly 3 weeks (Figure 4C). qRT-PCR confirmed sustainable miR203 expression in the AKT/Ras/miR203 group mouse livers (Figure 4D). However, no difference in mouse body weight or liver weight/body weight ratio between these two groups was observed (Figure 4E). This is possibly because body weight loss in AKT/Ras mice was compensated by increased tumor burden. IHC staining showed decreased expression of phosphorylated AKT, NRas, and Ki67 (Figure 4F). Likewise,

miR203 also suppressed the development of AKT/h-Met-induced HCC (Figure 4G). AKT/h-Met-treated mice died within 50 days postinjection, whereas AKT/h-Met/miR203 mice survived up to 92 days (Figure 4H). Upregulation of miR203 level was verified in the miR203 treated AKT/h-Met mice (Figure 4I). Interestingly, the liver weight/body weight ratio was significantly reduced in the AKT/h-Met/miR203 group mice because of the minor tumor burden (Figure 4J). Therefore, these data clarified that miR203 appears to be a robust tumor suppressor in HCC initiation and progression *in vivo*.

miR203 targets NRas and downstream cascade proteins in HCC

To screen possible targets of miR203 in HCC, we performed RNA-Seq using AKT/Ras and AKT/Ras/miR203 mouse HCC or liver tissues.

miR-203 inhibits hepatocellular carcinoma by targeting NRas

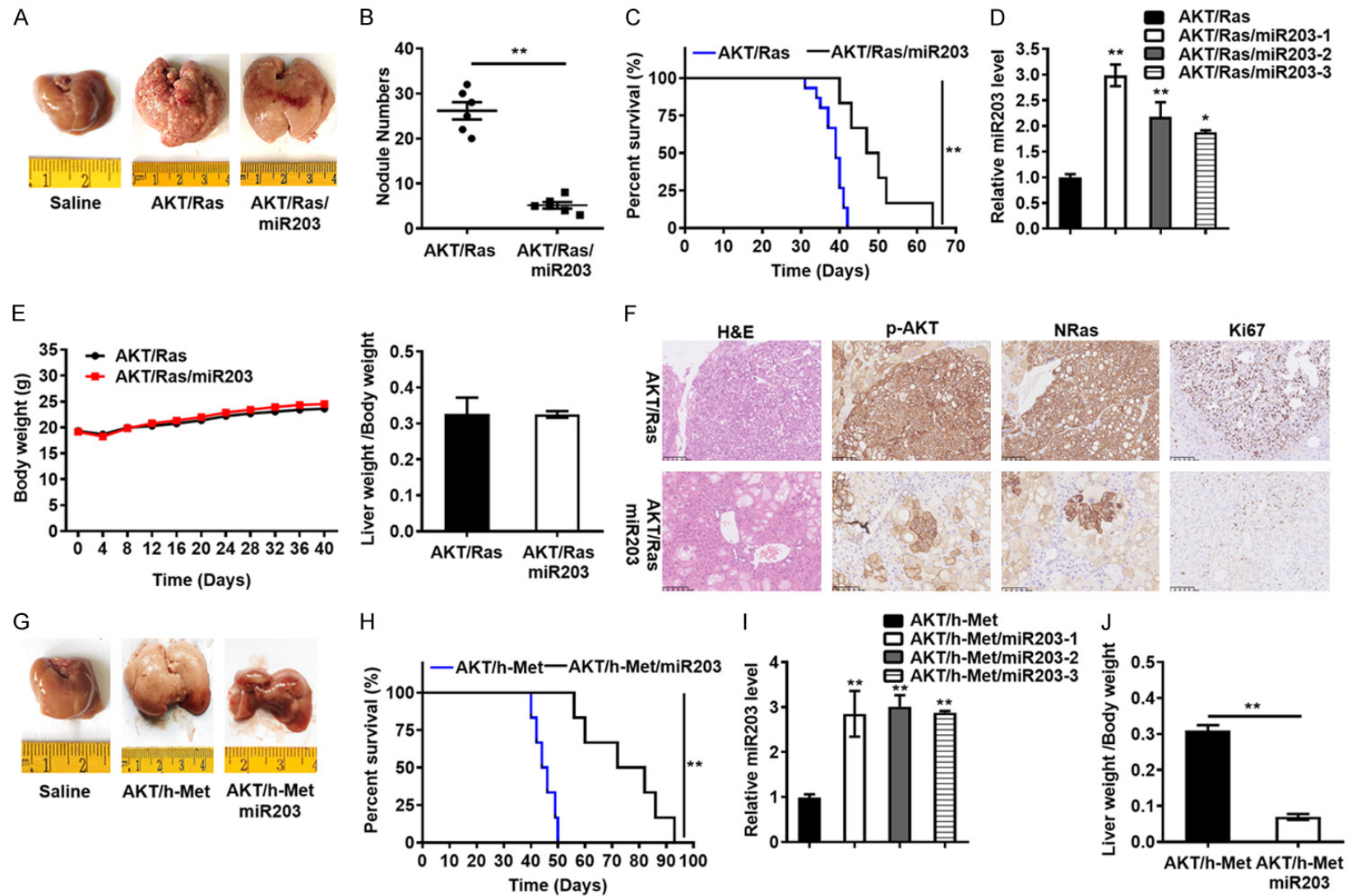


Figure 4. miR203 overexpression inhibits the development of HCC induced by AKT/Ras and AKT/h-Met. A. Representative liver images of livers from AKT/Ras mice (n = 6) and AKT/Ras/miR203 mice (n = 6). B. Liver tumor numbers in mice injected with AKT/Ras (n = 6) or AKT/Ras/miR203 (n = 6). C. Kaplan-Meier survival curves of the AKT/Ras (n = 15) and AKT/Ras/miR203 (n = 15) mouse cohorts. D. miR203 level in each group by qRT-PCR. E. Body weight and liver/body weight ratio of AKT/Ras or AKT/Ras/miR203 mice (n = 6). F. Microscopic appearance and immunohistochemistry (IHC) staining of liver tissues from each group. G. Macroscopic appearance of livers from AKT/h-Met mice (n = 6) and AKT/h-Met/miR203 mice (n = 6). H. Survival curves of the AKT/h-Met and AKT/h-Met/miR203 mice. I. miR203 level in each group by qRT-PCR. J. Liver/body weight ratio of AKT/h-Met and AKT/h-Met/miR203 mice. Data represent mean \pm SEM. * P < 0.05, ** P < 0.01. Scale bar = 100 μ m, magnification = 200 \times .

miR-203 inhibits hepatocellular carcinoma by targeting NRas

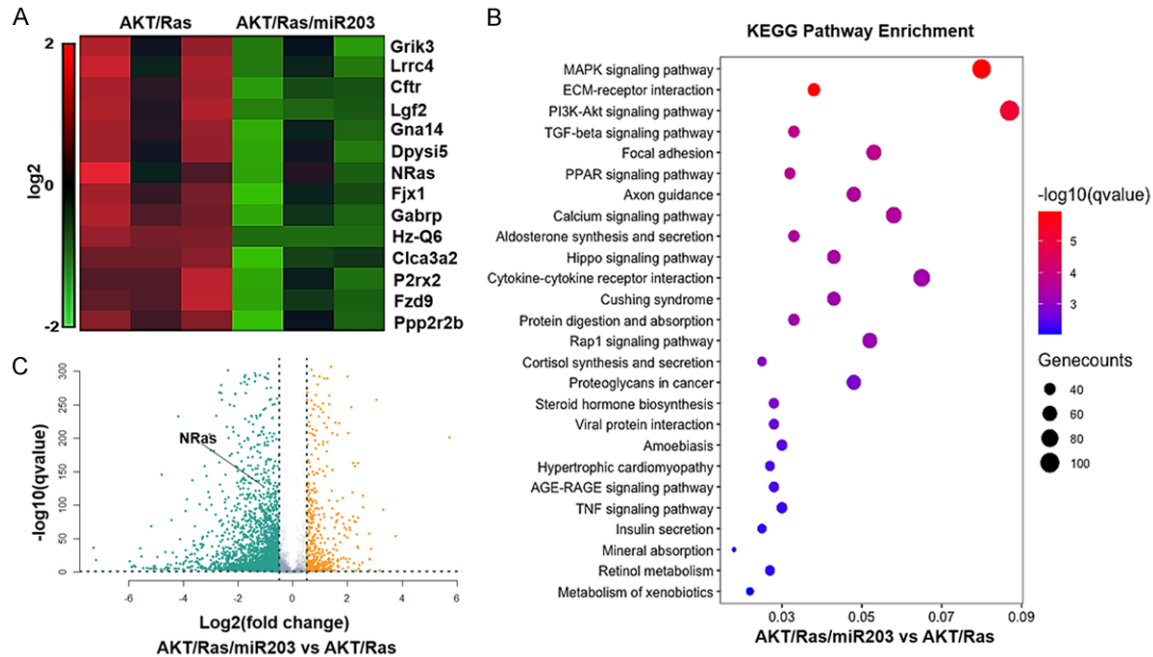


Figure 5. Microarray analysis indicates NRas as a downstream target of miR203 in HCC. A. Heatmap of the differentially expressed genes with a fold-change > 2 and $P < 0.05$ between AKT/Ras and AKT/Ras/miR203 mouse liver tissues ($n = 3$, red = upregulation, green = downregulation). B. KEGG signaling pathway enrichment in AKT/Ras/miR203 mice versus AKT/Ras mice ($n = 3$) using DAVID analysis. C. Volcano plot of all differentially expressed genes in AKT/Ras/miR203 mice versus AKT/Ras mice ($n = 3$, orange = upregulation, green = downregulation).

We selected genes with a fold-change > 2 and a P value < 0.05 among the AKT/Ras and AKT/Ras/miR203 groups. The top 14 genes were listed and analyzed using a heatmap ($n = 3$, red = upregulation, green = downregulation) (Figure 5A). KEGG pathway enrichment showed the enrichment of the MAPK signaling pathway, and several gene counts in the MAPK signaling pathway were at maximum (Figure 5B). A volcano plot of all differentially expressed genes in AKT/Ras/miR203 mice versus AKT/Ras mice ($n = 3$, orange = upregulation, green = downregulation) indicated a 2-fold decrease in the NRas gene, illustrating that miR203 may target NRas (Figure 5C).

Next, we performed TargetScan analysis and found that miR203 binding sites were within the 3'UTRs of the NRas gene and were conserved in humans (Figure 6A). To confirm that miR203 directly binds the 3'UTRs of NRas, we performed a luciferase assay, and the results showed that cotransfection with LV3-miR203 significantly decreased the luciferase activity of the reporter vector with NRas 3'UTRs in Hep3B cells. In addition, mutation of miR203 binding sites within the 3'UTRs of NRas completely

abolished the inhibitory effect of miR203 on luciferase activity (Figure 6B). Next, we examined the inhibitory role of miR203 on Ras in HCC mouse models. The results showed that overexpression of miR203 in AKT/Ras-induced mouse HCC robustly decreased NRas expression at both the mRNA and protein levels. Moreover, activation of downstream MAPK cascade proteins was inhibited as well (Figure 6C, 6D). Western blotting further confirmed the inhibition of miR203 on Ras/MAPK signaling in human HCC cell lines and in AKT/h-Met-induced mouse HCC tissues (Figure 6E, 6F). The relative expression of all proteins was quantified (Figure S2). Together, these results demonstrate that NRas is a direct target of miR203 in HCC both *in vitro* and *in vivo*.

Ectopic expression of NRas rescues the growth inhibition caused by miR203

Then, we verified whether activation of Ras/MAPK signaling can restore growth inhibition by miR203 overexpression. In Huh7 cells, miR203 treatment led to evident cell death, whereas cells transfected with NRas (exogenously transfected) showed increased cell via-

miR-203 inhibits hepatocellular carcinoma by targeting NRAs

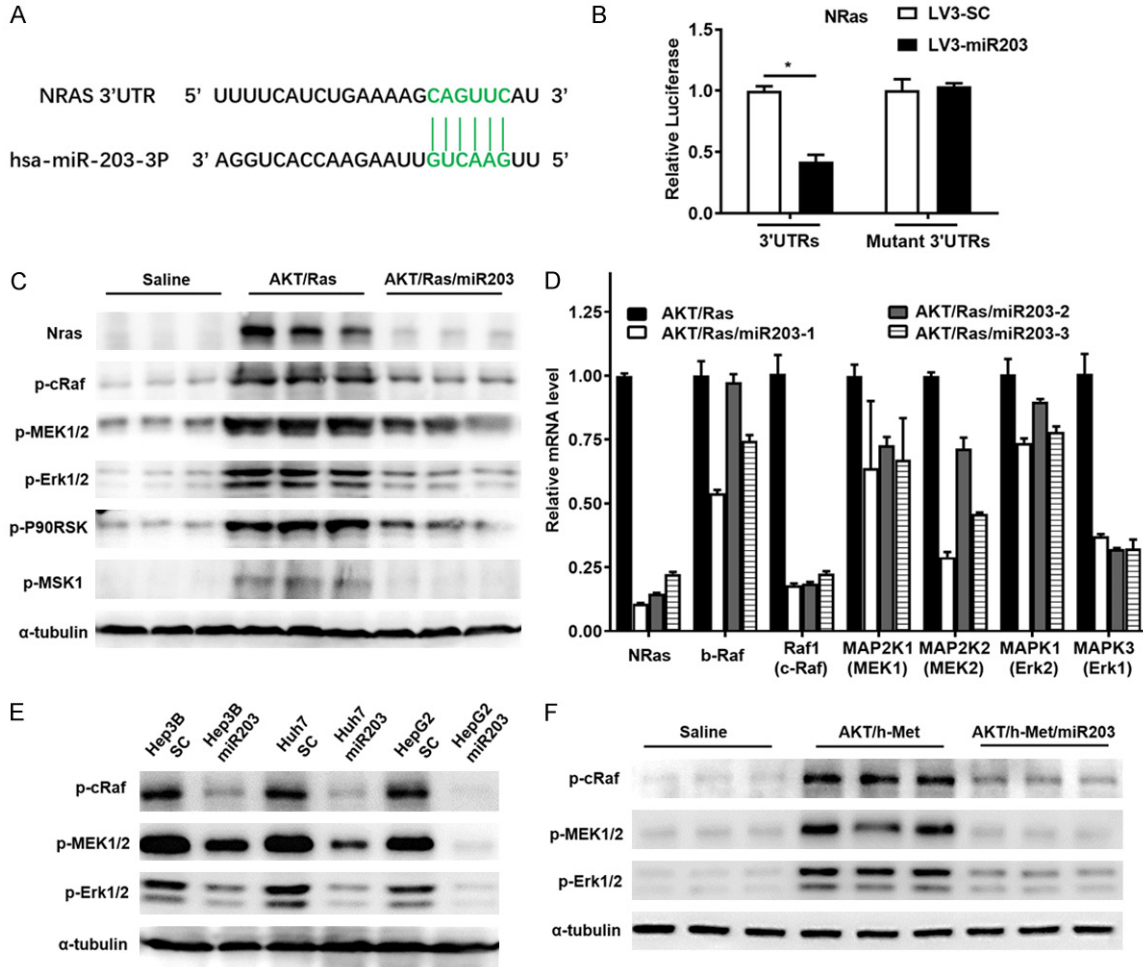


Figure 6. NRAs is the direct target of miR203. A. Schematic representation of the conserved miR203 binding motifs within the 3'-UTRs of miR203. Complementary sequences to the seed regions of miR203 within the 3'-UTRs are highlighted in green. B. Luciferase reporter analysis containing either the WT or mutated 3'-UTRs of human NRAs after transfection with LV3-miR203 or LV3-SC in Huh7 cells. C, D. Western blotting and qRT-PCR analysis of NRAs and Ras/MAPK signaling pathway-related genes. E, F. Western blotting analysis of Ras/MAPK-related proteins in HCC cells or AKT/h-Met-induced HCC mice after miR203 overexpression.

bility. Importantly, NRAs transfection recovered the cell viability reduced by miR203 at 4 days and 6 days (**Figure 7A**). The cell proliferation curve also confirmed the rescue function of ectopic NRAs expression (**Figure 7B**). Colony formation assays indicated that increased colony numbers were decreased by miR203 but were recovered by NRAs transfection (**Figure 7C**). Collectively, this evidence indicates that miR203 represses HCC cell growth by repressing the Ras/MAPK signaling pathway (**Figure 8**).

Discussion

In the present study, we found that miR203 was significantly downregulated in HCC cell

lines and clinical samples. Overexpression of miR203 inhibited cell growth and induced cell cycle arrest. Intriguingly, miR203 blocks the Ras/MAPK pathway by directly binding to the NRAs promoter. Critically, miR203 significantly inhibited the development of HCC in mice induced by AKT/Ras or AKT/h-Met coexpression. Therefore, our study revealed the tumor suppressive role of miR203 in HCC via repression of the Ras/MAPK signaling pathway.

Our results have several implications. First, this study provides robust evidence to support the tumor suppressive role of miR203 in hepatic carcinogenesis. Previous studies have demonstrated that miR203 acts as a tumor suppres-

miR-203 inhibits hepatocellular carcinoma by targeting NRas

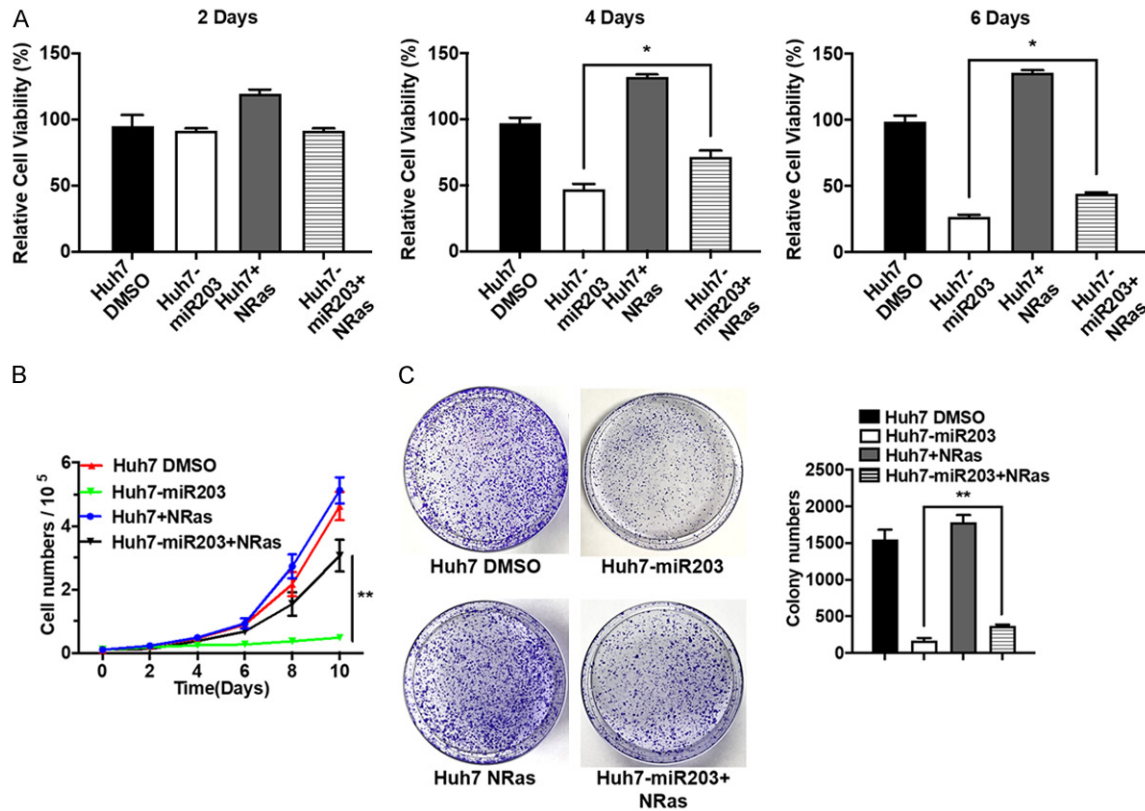


Figure 7. Ectopic expression of NRas can restore the inhibitory effect of miR203 on the proliferation of Huh7 cells. A. Cell viability analysis of Huh7 cells treated with DMSO, miR203 lentivirus, NRas, and miR203 lentivirus+ NRas at different time points using a CCK-8 kit. B. Cell proliferation curves of Huh7 cells with different treatments. C. Soft agar colony formation of Huh7 cells in each group. Data are presented as the mean \pm SD, $n = 3$ per group, * $P < 0.05$, ** $P < 0.01$.

sor in HCC [30-38]. The expression of miR203 is significantly downregulated in HCC tissues compared to normal liver tissues, and low miR203 expression is related to poor prognosis in HCC patients [32, 37, 38]. Subsequent functional studies indicated that miR203 impacts the growth, aggressiveness, and EMT transformation and increases the radiosensitivity of HCC cells by targeting MAT2A, MAT2B, Survivin, EZH2, and Bmi-1 [33-35]. However, most of these studies were performed either *in vitro* or in xenograft mouse models and critical *in vivo* evidence is lacking. In this study, we demonstrated that miR-203 inhibited tumor growth in AKT/Ras and AKT/h-Met primary HCC mouse models. Our data thus provide more robust evidence supporting the idea that miR203 functions as a tumor suppressor in hepatic carcinogenesis.

Second, our findings demonstrate the potential of miR203 as a nucleotide drug for HCC treat-

ment. MicroRNAs have been widely tested in both preclinical and clinical studies as therapeutics for cancer treatment. A few miRNA drugs, such as miR-155 and miR-16, are under investigation in human clinical trials with promising results ahead [39]. However, the development of nucleotide drugs still lags behind that of small molecule drugs due to the lack of effective nucleotide molecules. In this study, our data clearly indicate that miR203 functions as an NRas inhibitor and that restoration of miR203 can inhibit HCC growth both *in vitro* and *in vivo*. Notably, our data demonstrated that miR203 has the capacity to effectively inhibit the development of HCC in AKT/Ras and AKT/Met HCC mouse models. Therefore, our findings suggest that miR203 may serve as an ideal miRNA drug for the treatment of HCC.

Moreover, our study reveals that miR203 may serve as an inherently effective Ras inhibitor. Mounting evidence indicates that the Ras/

miR-203 inhibits hepatocellular carcinoma by targeting NRAs

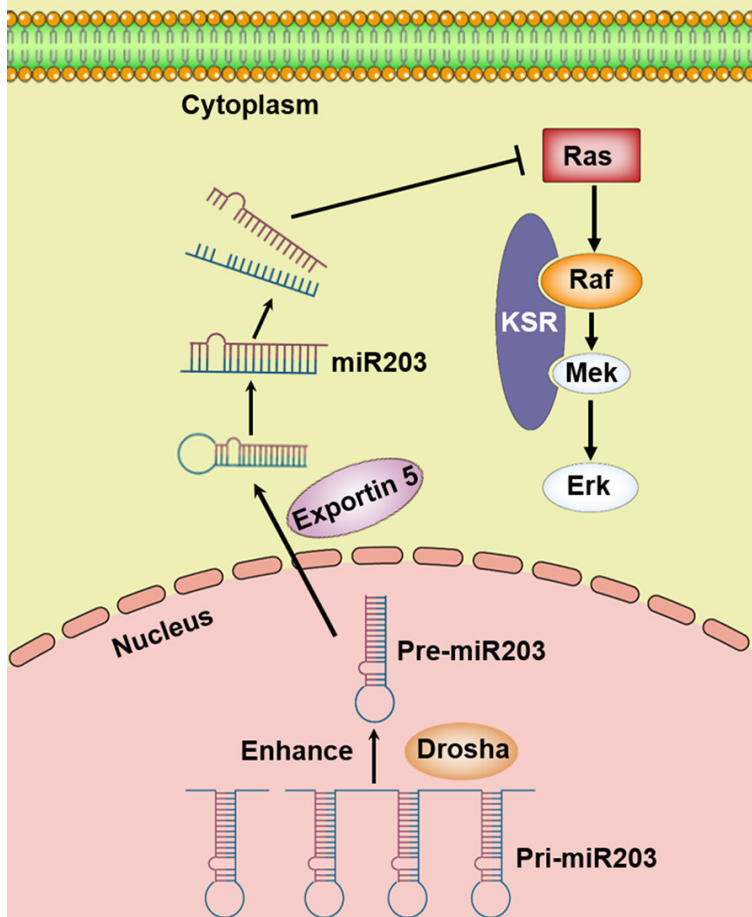


Figure 8. Schematic representation of the role of the Ras/MAPK signaling pathway in miR203-mediated repression of HCC development.

MAPK signaling pathway plays a major role in the malignant transformation and progression of HCC [9]. Blockade of the Ras/MAPK pathway is an important strategy for HCC treatment. Although many Raf, MEK, or ERK inhibitors are under clinical trials for HCC treatment, the discovery and development of Ras inhibitors were retarded for many years until the discovery of AMG-510 [16]. Intriguingly, our study indicates that miR-203 is a natural inhibitor of Ras signaling. A luciferase reporter assay demonstrated that miR-203 directly binds to the 3'UTR of NRAs. Overexpression of miR203 significantly decreased both the protein and mRNA levels of NRAs and molecules associated with the Ras/MAPK signaling pathway *in vitro* and *in vivo*. Restoration of Ras/MAPK signaling can completely reverse the growth inhibition caused by miR203 overexpression since exogenously introduced NRAs lacks a natural 3'UTR and hence cannot be blocked by miR203. Therefore, inherent NRAs was blocked, but exoge-

nous NRAs rescued HCC cell growth. Together, our results suggest that miR203 is an inherent Ras inhibitor and thus can be used for the treatment of HCC with activated Ras/MAPK signaling.

Our study has several limitations. First, the effects of miR203 delivery were only examined in cell line-derived xenograft (CDX) and primary HCC mouse models but not in patient-derived xenograft (PDX) models. It is known that PDX models harbor similar genetic alterations and full immune and stromal microenvironments to human HCC tissues. However, due to technical limitations, we failed to investigate the effects of miR203 in PDX HCC models. The second limitation is that we did not evaluate the effects of miR203 in HCC mouse models with different Ras mutations. In this study, we tested the effects of miR203 in AKT/Ras (NRasV12) and AKT/Met mouse models.

Whether miR203 treatment is effective for HCC with other mutations needs to be further confirmed. Finally, we did not evaluate the systemic toxicity of miR-203 administration in mice. In addition to cancer, miR203 also plays roles in other tissues or organs. Whether systemic delivery of miR203 causes severe adverse effects should be investigated.

Acknowledgements

This study was supported by the National Foundation of Science of China (81702448, 82273059, and 82073091), the Joint Foundation of Health Commission of Hubei Province (WJ2019H436) and the key Research and Development Program of Shaanxi Province, China (Grant No. 2017SF-200).

Disclosure of conflict of interest

None.

Address correspondence to: Dr. Xiaolei Li, Department of Thyroid and Breast Surgery, The 960th Hospital of The PLA, Jinan 250031, Shandong, China. E-mail: xiaolei86@126.com; Dr. Chuanrui Xu, School of Pharmacy, Tongji Medical College, Huazhong University of Science and Technology, Wuhan 430030, Hubei, China. E-mail: xcr@hust.edu.cn

References

- [1] Sung H, Ferlay J, Siegel RL, Laversanne M, Soerjomataram I, Jemal A and Bray F. Global cancer statistics 2020: GLOBOCAN estimates of incidence and mortality worldwide for 36 cancers in 185 countries. *CA Cancer J Clin* 2021; 71: 209-249.
- [2] El-Serag HB and Rudolph KL. Hepatocellular carcinoma: epidemiology and molecular carcinogenesis. *Gastroenterology* 2007; 132: 2557-2576.
- [3] Farazi PA and DePinho RA. Hepatocellular carcinoma pathogenesis: from genes to environment. *Nat Rev Cancer* 2006; 6: 674-687.
- [4] Younossi ZM and Henry L. Epidemiology of non-alcoholic fatty liver disease and hepatocellular carcinoma. *JHEP Rep* 2021; 3: 100305.
- [5] Valery PC, Laversanne M, Clark PJ, Petrick JL, McGlynn KA and Bray F. Projections of primary liver cancer to 2030 in 30 countries worldwide. *Hepatology* 2018; 67: 600-611.
- [6] Raoul JL, Frenel JS, Raimbourg J and Gilibert M. Current options and future possibilities for the systemic treatment of hepatocellular carcinoma. *Hepat Oncol* 2019; 6: HEP11.
- [7] Finn RS, Qin S, Ikeda M, Galle PR, Ducreux M, Kim TY, Kudo M, Breder V, Merle P, Kaseb AO, Li D, Verret W, Xu DZ, Hernandez S, Liu J, Huang C, Mulla S, Wang Y, Lim HY, Zhu AX and Cheng AL; IMbrave150 Investigators. Atezolizumab plus bevacizumab in unresectable hepatocellular carcinoma. *N Engl J Med* 2020; 382: 1894-1905.
- [8] Gordan JD, Kennedy EB, Abou-Alfa GK, Beg MS, Brower ST, Gade TP, Goff L, Gupta S, Guy J, Harris WP, Iyer R, Jaiyesimi I, Jhaver M, Karippot A, Kaseb AO, Kelley RK, Knox JJ, Kortmansky J, Leaf A, Remak WM, Shroff RT, Sohal DPS, Taddei TH, Venepalli NK, Wilson A, Zhu AX and Rose MG. Systemic therapy for advanced hepatocellular carcinoma: ASCO guideline. *J Clin Oncol* 2020; 38: 4317-4345.
- [9] Delire B and Stärkel P. The Ras/MAPK pathway and hepatocarcinoma: pathogenesis and therapeutic implications. *Eur J Clin Invest* 2015; 45: 609-623.
- [10] Schmidt CM, McKillop IH, Cahill PA and Sitzmann JV. Increased MAPK expression and activity in primary human hepatocellular carcinoma. *Biochem Biophys Res Commun* 1997; 236: 54-58.
- [11] Huynh H, Nguyen TT, Chow KH, Tan PH, Soo KC and Tran E. Over-expression of the mitogen-activated protein kinase (MAPK) kinase (MEK)-MAPK in hepatocellular carcinoma: its role in tumor progression and apoptosis. *BMC Gastroenterol* 2003; 3: 19.
- [12] Tsuboi Y, Ichida T, Sugitani S, Genda T, Inayoshi J, Takamura M, Matsuda Y, Nomoto M and Aoyagi Y. Overexpression of extracellular signal-regulated protein kinase and its correlation with proliferation in human hepatocellular carcinoma. *Liver Int* 2004; 24: 432-436.
- [13] Calvisi DF, Pinna F, Meloni F, Ladu S, Pellegrino R, Sini M, Daino L, Simile MM, De Miglio MR, Virdis P, Frau M, Tomasi ML, Seddaiu MA, Muroli MR, Feo F and Pascale RM. Dual-specificity phosphatase 1 ubiquitination in extracellular signal-regulated kinase-mediated control of growth in human hepatocellular carcinoma. *Cancer Res* 2008; 68: 4192-4200.
- [14] Kim D, Xue JY and Lito P. Targeting KRAS(G12C): from inhibitory mechanism to modulation of antitumor effects in patients. *Cell* 2020; 183: 850-859.
- [15] McCormick F. Progress in targeting RAS with small molecule drugs. *Biochem J* 2019; 476: 365-374.
- [16] Hong DS, Fakih MG, Strickler JH, Desai J, Durm GA, Shapiro GI, Falchook GS, Price TJ, Sacher A, Denlinger CS, Bang YJ, Dy GK, Krauss JC, Kuboki Y, Kuo JC, Coveler AL, Park K, Kim TW, Barlesi F, Munster PN, Ramalingam SS, Burns TF, Meric-Bernstam F, Hearn H, Ngang J, Ngarmchamnanrith G, Kim J, Houk BE, Canon J, Lipford JR, Friberg G, Lito P, Govindan R and Li BT. KRAS(G12C) inhibition with sotorasib in advanced solid tumors. *N Engl J Med* 2020; 383: 1207-1217.
- [17] Tanaka N, Lin JJ, Li C, Ryan MB, Zhang J, Kiedrowski LA, Michel AG, Syed MU, Fella KA, Sakhi M, Baiev I, Juric D, Gainor JF, Klemperer SJ, Lennerz JK, Siravegna G, Bar-Peled L, Hata AN, Heist RS and Corcoran RB. Clinical acquired resistance to KRAS(G12C) inhibition through a novel KRAS switch-II pocket mutation and polyclonal alterations converging on RAS-MAPK reactivation. *Cancer Discov* 2021; 11: 1913-1922.
- [18] Zhu X, Er K, Mao C, Yan Q, Xu H, Zhang Y, Zhu J, Cui F, Zhao W and Shi H. miR-203 suppresses tumor growth and angiogenesis by targeting VEGFA in cervical cancer. *Cell Physiol Biochem* 2013; 32: 64-73.
- [19] Saini S, Majid S, Yamamura S, Tabatabai L, Suh SO, Shahryari V, Chen Y, Deng G, Tanaka Y and Dahiya R. Regulatory role of miR-203 in

miR-203 inhibits hepatocellular carcinoma by targeting NRas

- prostate cancer progression and metastasis. *Clin Cancer Res* 2011; 17: 5287-5298.
- [20] Viticchiè G, Lena AM, Latina A, Formosa A, Gregersen LH, Lund AH, Bernardini S, Mauriello A, Miano R, Spagnoli LG, Knight RA, Candi E and Melino G. MiR-203 controls proliferation, migration and invasive potential of prostate cancer cell lines. *Cell Cycle* 2011; 10: 1121-1131.
- [21] Li J, Zhang B, Cui J, Liang Z and Liu K. miR-203 inhibits the invasion and EMT of gastric cancer cells by directly targeting annexin A4. *Oncol Res* 2019; 27: 789-799.
- [22] Shen J, Zhang J, Xiao M, Yang J and Zhang N. miR-203 suppresses bladder cancer cell growth and targets twist1. *Oncol Res* 2018; 26: 1155-1165.
- [23] Zhang Z, Zhang B, Li W, Fu L, Fu L, Zhu Z and Dong JT. Epigenetic silencing of miR-203 up-regulates SNAIL2 and contributes to the invasiveness of malignant breast cancer cells. *Genes Cancer* 2011; 2: 782-791.
- [24] Zhou Y, Wan G, Spizzo R, Ivan C, Mathur R, Hu X, Ye X, Lu J, Fan F, Xia L, Calin GA, Ellis LM and Lu X. miR-203 induces oxaliplatin resistance in colorectal cancer cells by negatively regulating ATM kinase. *Mol Oncol* 2014; 8: 83-92.
- [25] Tao J, Ji J, Li X, Ding N, Wu H, Liu Y, Wang XW, Calvisi DF, Song G and Chen X. Distinct anti-oncogenic effect of various microRNAs in different mouse models of liver cancer. *Oncotarget* 2015; 6: 6977-6988.
- [26] Chen X and Calvisi DF. Hydrodynamic transfection for generation of novel mouse models for liver cancer research. *Am J Pathol* 2014; 184: 912-923.
- [27] Ng R, Wu H, Xiao H, Chen X, Willenbring H, Steer CJ and Song G. Inhibition of microRNA-24 expression in liver prevents hepatic lipid accumulation and hyperlipidemia. *Hepatology* 2014; 60: 554-564.
- [28] Ho C, Wang C, Mattu S, Destefanis G, Ladu S, Delogu S, Armbruster J, Fan L, Lee SA, Jiang L, Dombrowski F, Evert M, Chen X and Calvisi DF. AKT (v-akt murine thymoma viral oncogene homolog 1) and N-Ras (neuroblastoma ras viral oncogene homolog) coactivation in the mouse liver promotes rapid carcinogenesis by way of mTOR (mammalian target of rapamycin complex 1), FOXM1 (forkhead box M1)/SKP2, and c-Myc pathways. *Hepatology* 2012; 55: 833-845.
- [29] Hu J, Che L, Li L, Pilo MG, Cigliano A, Ribback S, Li X, Latte G, Mela M, Evert M, Dombrowski F, Zheng G, Chen X and Calvisi DF. Co-activation of AKT and c-Met triggers rapid hepatocellular carcinoma development via the mTORC1/FASN pathway in mice. *Sci Rep* 2016; 6: 20484.
- [30] Zheng XB, Chen XB, Xu LL, Zhang M, Feng L, Yi PS, Tang JW and Xu MQ. miR-203 inhibits augmented proliferation and metastasis of hepatocellular carcinoma residual in the promoted regenerating liver. *Cancer Sci* 2017; 108: 338-346.
- [31] Zhang A, Lakshmanan J, Motameni A and Harbrecht BG. MicroRNA-203 suppresses proliferation in liver cancer associated with PIK3CA, p38 MAPK, c-Jun, and GSK3 signaling. *Mol Cell Biochem* 2018; 441: 89-98.
- [32] Liu Y, Ren F, Rong M, Luo Y, Dang Y and Chen G. Association between underexpression of microRNA-203 and clinicopathological significance in hepatocellular carcinoma tissues. *Cancer Cell Int* 2015; 15: 62.
- [33] Wei W, Wanjun L, Hui S, Dongyue C, Xinjun Y and Jisheng Z. miR-203 inhibits proliferation of HCC cells by targeting survivin. *Cell Biochem Funct* 2013; 31: 82-85.
- [34] Simile MM, Peitta G, Tomasi ML, Brozzetti S, Feo CF, Porcu A, Cigliano A, Calvisi DF, Feo F and Pascale RM. MicroRNA-203 impacts on the growth, aggressiveness and prognosis of hepatocellular carcinoma by targeting MAT2A and MAT2B genes. *Oncotarget* 2019; 10: 2835-2854.
- [35] Shao Y, Zhang D, Li X, Yang J, Chen L, Ning Z, Xu Y, Deng G, Tao M, Zhu Y and Jiang J. MicroRNA-203 increases cell radiosensitivity via directly targeting BMI-1 in hepatocellular carcinoma. *Mol Pharm* 2018; 15: 3205-3215.
- [36] Chen XB, Zheng XB, Cai ZX, Lin XJ and Xu MQ. MicroRNA-203 promotes liver regeneration after partial hepatectomy in cirrhotic rats. *J Surg Res* 2017; 211: 53-63.
- [37] Chen HY, Han ZB, Fan JW, Xia J, Wu JY, Qiu GQ, Tang HM and Peng ZH. miR-203 expression predicts outcome after liver transplantation for hepatocellular carcinoma in cirrhotic liver. *Med Oncol* 2012; 29: 1859-1865.
- [38] Chen H, Kong M, Chen Y, Jiang Y, Wen M and Zhang X. Prognostic significance of miR-203 and ZEB1 expression in early-stage hepatocellular carcinoma. *J Cancer* 2021; 12: 4810-4818.
- [39] Romano G, Acunzo M and Nana-Sinkam P. microRNAs as novel therapeutics in cancer. *Cancers (Basel)* 2021; 13: 1526.

miR-203 inhibits hepatocellular carcinoma by targeting NRas

Table S1. Primers used for qRT-PCR

Gene	Sequence
<i>GAPDH (h)</i>	F 5'-GGAGCGAGATCCCTCCAAAAT-3' R 5'-GGCTGTTGTCATACTTCTCATGG-3'
<i>GAPDH (m)</i>	F 5'-AGGTCGGTGTGAACGGATTG-3' R 5'-TGTAGACCATGTAGTTGAGGTCA-3'
<i>U6 (h)</i>	F 5'-CGCTTCGGCAGCACATATAC-3' R 5'-TTCACGAATTTGCGTGTCAT-3'
<i>U6 (m)</i>	F 5'-CTCGCTTCGGCAGCACA-3' R 5'-AACGCTTCACGAATTTGCGT-3'
<i>miR-203 (h)</i>	F 5'-GTGAAATGTTTAGGACCACTAGAA-3' R 5'-GCTGTCAACGATACGCTACGT-3'
<i>miR-203 (m)</i>	F 5'-GCTGGGTCCAGTGGTTCTTA-3' R 5'-GCCGGGTCTAGTGGTCCTAA-3'
<i>NRas (m)</i>	F 5'-ACTGAGTACAACTGGTGGTGG-3' R 5'-TCGGTAAGAATCCTCTATGGTGG-3'
<i>b-Raf (m)</i>	F 5'-AATTTGGTGGAGAGCATAACCC-3' R 5'-ACGGTGTCCATTGATGCAGAG-3'
<i>Raf1 (m)</i>	F 5'-AGGGTGGTGAATTACAGCAA-3' R 5'-GCAGTGTAGAAAGCTGGAGAG-3'
<i>MAP2K1 (m)</i>	F 5'-AACGGTGGAGTGGTCTTCAAG-3' R 5'-CGGATTGCGGGTTTGTATCTC-3'
<i>MAP2K2 (m)</i>	F 5'-GTTACCGGCACTCACTATCAAC-3' R 5'-GCTCACCGACCTTAGCCTTC-3'
<i>MAPK1 (m)</i>	F 5'-TCAGATGAATTTTCGTTGGCAGA-3' R 5'-AGCTTTTGTATTGGTCACAGCA-3'
<i>MAPK3 (m)</i>	F 5'-TCCGCCATGAGAATGTTATAGGC-3' R 5'-GGTGGTGTGATAAGCAGATTGG-3'

Table S2. Antibodies used for Western blotting and immunohistochemistry

Antigen	Dilution	Isotype	Supplier	Catalogue number
For western blotting				
α -tubulin	1:1000	Rabbit IgG	BOSTER	BM1452
CyclinD1	1:1000	Rabbit IgG	BOSTER	BM0771
CyclinB1	1:1000	Rabbit IgG	BOSTER	BM4370
NRas	1:1000	Rabbit IgG	Proteintech	10724-1-AP
p-cRaf	1:1000	Rabbit IgG	Cell Signaling	9421
pAKT	1:1000	Rabbit IgG	Cell Signaling	4060
p-MEK1/2	1:1000	Rabbit IgG	Cell Signaling	2338
p-Erk1/2	1:1000	Rabbit IgG	Cell Signaling	4695
p-P90RSK	1:1000	Rabbit IgG	Cell Signaling	8753
p-MSK1	1:1000	Rabbit IgG	Cell Signaling	9595
For immunohistochemistry				
Ki67	1:200	Rabbit IgG	Cell Signaling	12202
NRas	1:200	Rabbit IgG	Proteintech	10724-1-AP
pAKT	1:100	Rabbit IgG	Cell Signaling	4060

miR-203 inhibits hepatocellular carcinoma by targeting NRas

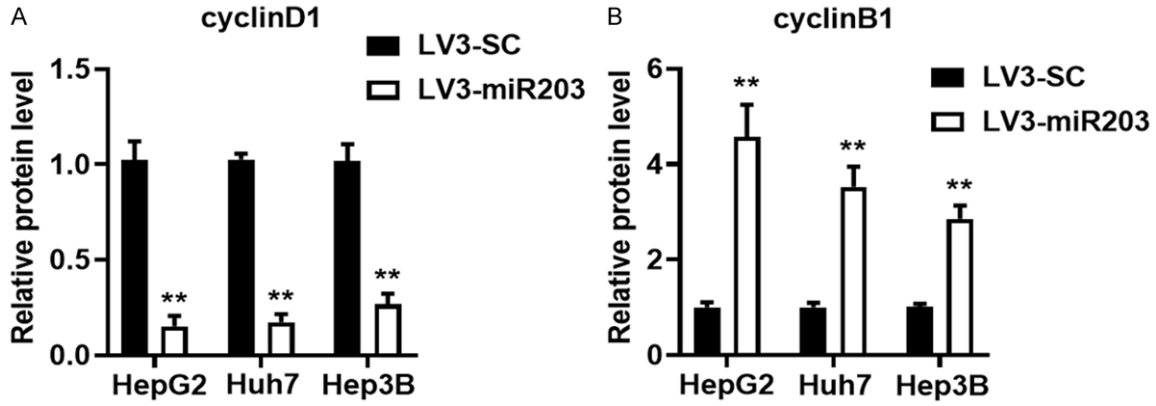


Figure S1. The expression of all cell cycle related proteins were quantified. (A) The relative protein level of cyclinD1. (B) The relative protein level of cyclinB1.

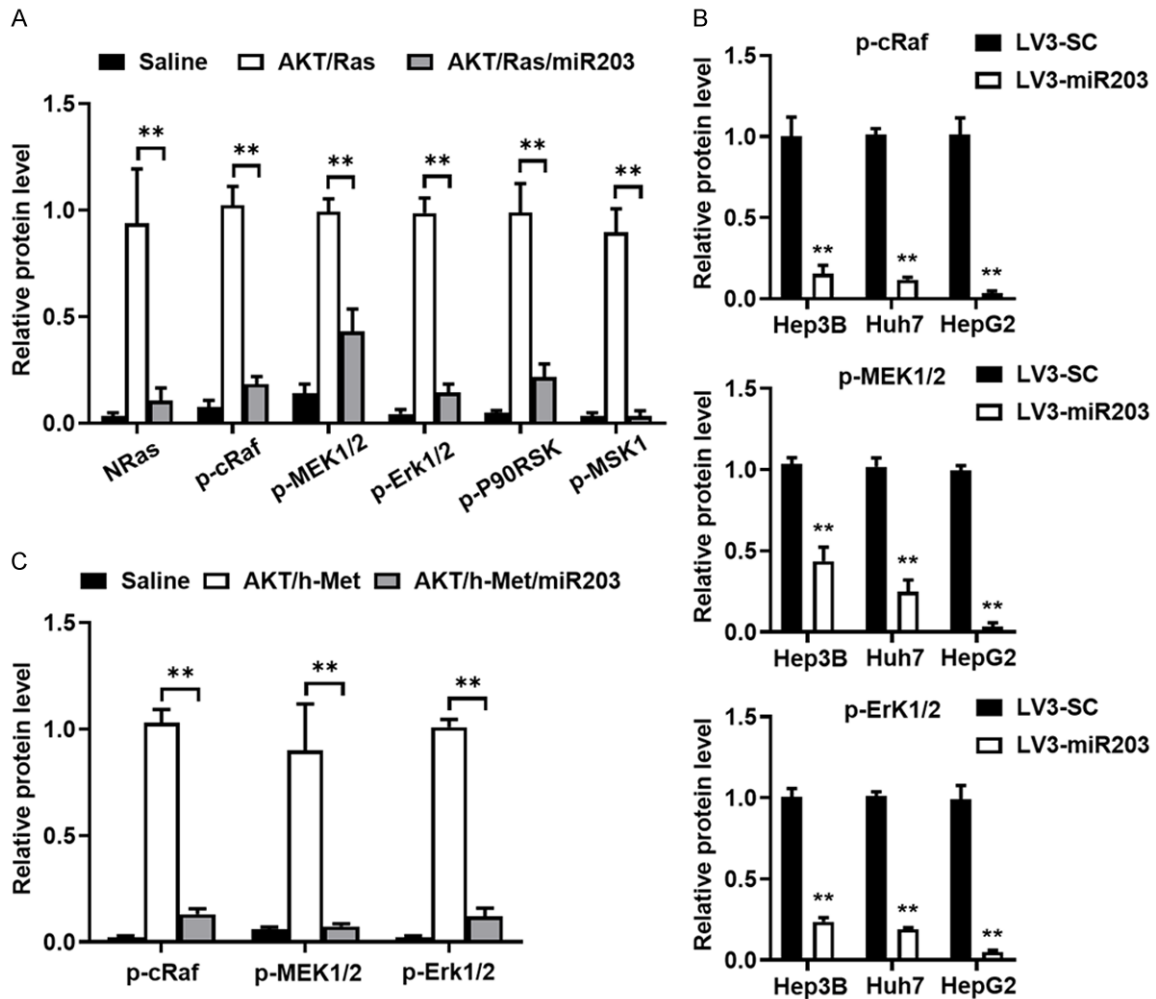


Figure S2. The relative expression of all Ras/MAPK signaling related proteins was quantified. (A) Relative protein levels of related proteins in AKT/Ras or AKT/Ras/miR203 mice liver tissues. (B) Relative protein levels of related proteins in HCC cells or miR203 overexpressed HCC cells. (C) Relative protein levels of related proteins in AKT/h-Met or AKT/Met/miR203 mice liver tissues.